JOURNAL OF CATALYSIS 138, 640–658 (1992)

Characterisation of Unsupported FeMoS Catalysts: Stability during Reaction and Effect of the Sulfiding Temperature

M. KARROUA,[1] J. LADRIÈRE, H. MATRALIS, P. GRANGE, AND B. DELMON

Unité de Catalyse et Chimie des Matériaux Divisés, Université Catholique de Louvain, Place Croix du Sud 2, Boîte 17, 1348 Louvain-la-Neuve, Belgium

Received July 29, 1991; revised May 7, 1992

Unsupported iron, molybdenum and iron-molybdenum sulfides were prepared by the Homogeneous Sulfide Precipitation (HSP) method. They were investigated by surface area, XRD, MAS (Mössbauer Absorption Spectroscopy), electrophoretic migration, and XPS measurements; various temperature-programmed methods have also been used. Catalytic activity in the simultaneous hydrodesulfurisation of thiophene and hydrogenation of cyclohexene at 3 MPa and 573 K has been measured. It has been verified that the HSP method gives samples containing a high proportion of the Fe species giving the signal attributed to the so called "FeMoS" species, together with a noncrystalline phase possibly corresponding to FeS_2 (pyrite) and some pyrrhotite ($Fe_{1-x}S$). When the final reduction–sulfidation (15% H_2S in H_2) temperature of the HSP precipitate is increased (from 673 to 1073 K), FeS_2 and the iron of FeMoS transform to troilite (FeS). Samples sulfided above 873 K no longer contain FeMoS. The FeMoS "phase" decomposes extensively during the catalytic reaction. Catalytic activity does not correlate with the quantity of FeMoS present in the samples, but seems to vary in parallel with the amount of FeS_2 remaining in the working catalyst.

INTRODUCTION

Transition metal sulfide catalysts are widely used in the oil-processing industry for the removal of environmentally harmful hetero-atoms, like sulfur (hydrodesulfurisation, HDS) and nitrogen, from crude oil fractions or coal-derived liquids. Catalysts consisting of molybdenum sulfide promoted by cobalt or nickel sulfide supported on porous alumina are most commonly applied. But iron sulfides (pyrite, pyrrhotite, etc.) also play some role. Alone, they can accelerate coal hydroconversion (*1, 2*). Investigations concerning various possible processes for coal liquefaction and refining of coal-derived products have laid emphasis on catalysts containing iron sulfide (*3–5*). Iron sulfide might also replace cobalt or nickel sulfide as a low cost promoter of molybdenum in more conventional hydrotreating processes.

In the last 10 years, attempts have been made to elucidate the promoter effect of Fe on the HDS activity of MoS_2, but the results do not offer a clear picture of the role of Fe. Thakur *et al.* (*6*) compared the activity in the HDS of thiophene and the hydrogenation (HYD) of cyclohexene, of MoS_2 and WS_2 promoted by Co, Ni, or Fe. They found the promoter action of Ni and Co to be much more pronounced than that of Fe for both reactions. Other workers (*7–10*) also reported that the HDS activity of MoS_2 is only weakly promoted by iron. In the work of Ramselaar *et al.* (*11, 12*), it was found that the HDS activity of MoS_2 supported on carbon was increased by a factor of 1.2 when iron was added to the formulation. Vaishnava *et al.* (*4*) studied a series of alumina-supported FeMo catalysts with different Fe/Mo ratios. They found that the addition of a small amount of iron to Mo/Al_2O_3 cata-

[1] Present address: Mohamed 1er Université, Oujda, Morocco.

0021-9517/92 $5.00

TABLE 1

Reported Mössbauer Absorption Spectroscopy Parameters of the "FeMoS Species"

Sulfide	QS (mm/s)	IS (mm/s)	References
FeMo/C	1.04	0.63	(*11, 12*)
$FeMo/Al_2O_3$	0.84	0.30	(*14, 16*)
$FeMo/Al_2O_3$	0.78	0.35	(*17*)
FeMo	0.99–1.22	0.30–0.35	(*18, 19*)

lysts considerably lowered activity, while at higher Fe contents, the activity was approximately equal to the sum of those of the individual components. These studies did not permit identification of the nature of the active phase or phases operating in the FeMo catalysts. A special MES signal (Mössbauer Emission Spectroscopy) is detected in the similar CoMo catalysts, supported or unsupported, when fresh (*13, 14*). This special signal has been attributed to an amorphous "CoMoS phase," which was considered to be the phase possessing the highest HDS activity (*15*). A similar signal, believed to come from a similar "FeMoS phase" has been found in Mössbauer Absorption Spectroscopy (MAS) in both supported (*11, 12, 14–17*) or unsupported (*13, 18, 19*) FeMo catalysts. The "FeMoS phase" MAS signal was characterised by the values of the electrical quadrupole splitting (QS) and isomer shift (IS) reported in Table 1. According to Topsøe *et al.* (14), the HDS activity of the iron-promoted $FeMo/Al_2O_3$ catalysts is lower than that of those containing only MoS_2, in spite of the presence of the "FeMoS phase." In opposition with this Qi *et al.* (*17*) and Ramselaar (*12*) found that the HDS activity of FeMo supported on alumina or carbon correlates with the amount of "FeMoS phase" in the fresh catalyst. Some studies (*4, 8, 10, 20*) reported that pure iron sulfide, i.e., iron sulfide not associated in any mixed phase with Mo, could slightly promote HDS activity.

Several hypotheses concerning the role of separate iron sulfide have been proposed: (i) pure iron sulfide activates the Mo sites thanks to the action of a mobile species, namely, hydrogen spill-over, that it produces (*20*); or (ii) the fact that iron sulfide slightly alters the electronic configuration of MoS_2 (*6, 8, 10*); or (iii) the possibility that pure iron sulfide, namely, FeS_2 or FeS alone, would be able to catalyse the hydrogenolysis and hydrogenation reactions (*12, 21*).

The aim of the present work is to contribute to evaluating the validity of these respective views.

The HDS activity of the "FeMoS" phase was mostly studied under atmospheric pressure and this phase was reported to be stable (*12*). Generally, however, the metal (Me) in the "decoration" positions on the MoS_2 edges in the "MeMoS structure" seems to have a low stability and it tends to segregate into pure Me sulfide (*22, 23*). The extent of segregation is more pronounced when the "MeMoS phase" is tested under high H_2 pressure (*24, 25*). Correlations between activity and structure should thus be sought using catalysts subjected to the conditions generally used in HDS and HYD. Used catalysts protected from any contact with reactive molecules should possess a structure closely related (or identical) to that of the working catalyst. They should be used preferentially if measurements during the catalytic reaction are too difficult. This is what we did.

In the reports mentioned in the literature, the Fe content has been varied quite often in order to find if some correlation existed between the activity and the structural properties of the active phase. The sulfiding temperature is also an important factor which can influence the textural and structural properties of the active phase in the catalysts. For the present work, we prepared unsupported FeMo catalysts, containing 30 and 15% Fe atoms (in principle, these contents allow the greater part or, possibly, all the iron to be included in the "FeMoS phase"). Sulfidation temperatures ranging from 673 to 1073 K were used.

The so-called "FeMoS phase" (as well as "CoMoS" and "NiMoS"), in reality, is not well defined. Ledoux *et al.* suggested from NMR measurements that the distorted tetrahedral Co atoms upon adsorption of the sulfided molecule lead to octahedral "rapid" configuration, this stabilization being possible either in the CoMo phase or in small pores of the carbon support (*26–28*). The standard way in which the CoMoS and FeMoS associations are defined is actually indirect, i.e., by virtue of the special Mössbauer signal they give (the situation is still more complicated in the case of NiMoS). For these reasons, many investigations have been conducted to find other characteristics distinguishing FeMoS (or CoMoS or NiMoS) from the corresponding pure phases (MoS_2, Co_9S_8, NiS_x, FeS, etc.) and their mixtures.

For the present work, much care has been taken to ensure that the "FeMoS" prepared should exhibit all the characteristics attributed to the "FeMoS phase" in the literature (*14, 17–19, 29–32*). To this end, the catalysts were characterized by DTA, microelectrophoresis, XRD, TPR, and MAS (Mössbauer Absorption Spectroscopy). The proportion of the "FeMoS phase" present in the catalysts was estimated from the intensity of the special MAS signal. XPS analysis of the catalysts was used to identify the iron surface species. The texture and structure of the fresh sulfides were studied by XRD, XPS, TPR, and MAS. In addition, XRD and MAS were used to analyse the tested (used) catalysts in order to detect the structural modifications which could occur during reaction. The hydrodesulfurisation (HDS) of thiophene and hydrogenation (HYD) of cyclohexene were used as model reactions. They were performed at 573 K and under a pressure of 3 MPa.

EXPERIMENTAL

Catalysts Preparation

Precursors. The precursors (precipitated oxysulfides) of pure MoS_2 and those of the "FeMoS" mixed sulfides (atomic ratios r = Fe : (Fe + Mo) = 0.15 and 0.30; notation: FeMoS − 0.15 and FeMoS − 0.30) were prepared according to the so-called homogeneous sulfide precipitation method (HSP) (*29, 30*). The procedure of preparation of the precursor of MoS_2 is described in Ref. (*24*). The precursor of "FeMoS" was prepared in the same way as those of "CoMoS" (24), using $Fe(NO_3)_3 \cdot 9H_2O$ as starting material. In addition, the pH of the solution containing Fe and Mo was kept equal to 1.5, by addition of the nitric acid. This is necessary in order to prevent the formation of a yellow precipitate before mixing with ammonium sulfide. The various stages (precipitation, evaporation and drying) were carried out under an Ar atmosphere. Pure iron sulfate ($FeSO_4 \cdot 7H_2O$) was used as the precursor of iron sulfide (hexagonal pyrrhotite $Fe_{1-x}S$).

Particles of sizes comprised between 200 and 400 μm were obtained by sieving, under air.

Sulfides. The unsupported MoS_2, $Fe_{1-x}S$, FeMoS − 0.15, and FeMoS − 0.30 sulfides were obtained by heating 4 g of their precursors in argon (100 ml min^{-1}) at 373 K for 1 h, then switching to an H_2S/H_2 (15% volume H_2S) mixture (100 ml min^{-1}) and increasing the temperature at a rate of 3.3 K min^{-1} up to 673 K. The temperature was then maintained at this level for 4 h. In addition, FeMoS-0.30 samples were also sulfided by the same H_2S/H_2 mixture at 773, 873, and 1073 K, all other experimental parameters being kept constant. The samples will be indicated as FeMoS-r-*T*, where r is the atomic ratio and *T* indicates the activation temperature in K (i.e., FeMoS-0.30-773 refers to FeMoS of composition r = 0.30 sulfided at 500°C).

Physico-chemical Characterization

The specific surface areas were measured using the BET method. The XRD spectra were obtained with a Kristalloflex 805 diffractometer (Siemens) with a highly sensitive detector (Siemens D-500), using Cu $K\alpha$ radiation. For the XRD measurements, the catalysts were stored in *n*-pentane in order

to protect them from oxidation. Precursors, sulfides, and solids resulting from temperature-programmed reaction (TPS and TPO) were studied. The thickness of the MoS_2 crystallites in the direction corresponding to the *c*-axis (002) of the FeMoS-0.30-*T* sulfides, was calculated using the formula (*33*)

$$D = 0.94\,\lambda/\beta\cos\theta,$$

where D is the lattice dimension (Å) along the *c*-axis, λ the wavelength (1.5418 Å) and β the corrected line-width in radians ($\beta = \beta'$ catalyst (measured) $- \beta''$ reference (measured)). Well-crystallized MoS_2 (Merck) was used as a reference. Mössbauer spectra (MAS) were recorded at 298 K, using a constant acceleration spectrometer equipped with a 12-mCi source of ^{57}Co in rhodium. Isomer shift (IS) was evaluated taking as a reference pure alpha-iron. The spectra were fitted by a sum of Lorentzian lines using an iterative nonlinear least-squares program. The relative amounts (*%I*) of compounds were computed from the peak areas, assuming that all species have similar Lamb–Mössbauer factors. The possible error on the relative amounts of the species, due to this assumption, is estimated to be less than ±5%. The estimated errors on the quadrupole splitting (QS), isomer shift (IS), and internal magnetic field (H_i) are, respectively, 0.05 mm/s, 0.05 mm/s, and 4 kOe.

For electrophoretic migration measurements, the sulfides were first ground and sieved under air in order to obtain particles of 25 μm and then subsequently resulfided. Their isoelectric points (IEP), as defined by Parks (*34*), were obtained by measuring the electrophoretic migration velocity in a Lazer-Zee Meter model 500 (Pen-Kem-In).

Temperature-programmed reactions of the precursors of the MoS_2, $Fe_{1-x}S$, and FeMoS-0.30-673 sulfides were carried out in a home-made, all glass, atmospheric pressure DTA apparatus, adapted to use with sulfur-containing substances. The heating rate and gas flow were equal to 10 K min^{-1} and 60 ml min^{-1}, respectively. The standard deviation of the reported temperatures is ±3 K. Three experimental procedures were followed. In the first one, the thermal decomposition of the precursor was conducted under Ar. When the maximum temperature (823 K) was reached, the samples were cooled to 673 K and maintained at this temperature for 2 h. Then they were cooled to room temperature and the temperature-programmed oxidation (TPO) of the resulting solid was performed using air as the reacting atmosphere. The second experimental procedure consisted of a temperature-programmed sulfidation-reduction (TPS) of the precursor (reaction atmosphere: H_2/H_2S, 15% vol. H_2S) followed by TPO as above. For temperature programmed reduction (TPR) measurements we made on sulfided phases without a previous TPO run (*32*); the H_2 flow rate was 40 ml min^{-1}.

XPS analysis was performed at room temperature with an SSX-100 model 206 Surface Science Instruments (SSI) photoelectron spectrometer using a monochromated Al anode (Al $K\alpha$, 1486.6 eV), powered at 10 kV and 20 mA, interfaced to a Hewlett–Packard 9000/310 computer. The residual pressure in the spectrometer was in the range 1×10^{-7} to 5×10^{-7} Pa. The positive charge developed on the samples was compensated for by a charge neutraliser (a flood gun) whose energy was adjusted to 6 eV and 50 μA. The intensities were estimated by calculating the integral of each peak after subtraction of the background, assumed to be "S-shaped" (*35*). Atomic concentration ratios were calculated by correcting the intensity ratios with the theoretical sensitivity factors based on the Scofield (*36*) cross sections, assuming the transmission function of the spectrometer to be independent of the kinetic energy (E_K). The electron mean free paths (IMFP) were assumed to vary as the function $(E_K)^{0.7}$. Decomposition of peaks was done with the best fitting routine of the SSI instrument. In order to avoid exposure of the sulfided samples to air, the catalysts were cooled to room temperature under a stream of Ar, covered with a meniscus of iso-octane, and

subsequently transferred into the spectrometer (*37*).

Catalytic Activity Measurements

The catalytic activity of MoS_2, $Fe_{1-x}S$, FeMoS-0.15, and FeMoS-0.30-*T* sulfides was measured. As model reactions were used the hydrodesulfurization of thiophene and the hydrogenation of cyclohexene, measured simultaneously. The activity measurements were performed in a stainless steel automatic high pressure "Catatest" apparatus (Géomécanique), working in the continuous flow regime. The reactant was a mixture of cyclohexane (70 wt%), cyclohexene (29.5 wt%) and 5000 ppm of thiophene. The flow rate of the liquid feed was 48 g h^{-1} corresponding to liquid hourly space velocities (LHSV) of 34 h^{-1}. The H_2 (gas N.T.P.)/hydrocarbon (liquid) ratio was 600. For all samples, the catalytic activity with 2 g of catalyst was measured at 573 K under a pressure of 3 MPa. As exposure to air during transfer into the reactor could not be avoided, the samples were resulfided in situ at 573 K for 1 h by a mixture of 15% (vol)H_2S/H_2. The liquid products were analysed every 1 h, for 12 h, using a gas chromatograph (Intersmat, IGC 121 DFL; the column was 10% Carbowax 20 m/Chromosorb). Activities were expressed as % conversion and as intrinsic activities, namely the amount of thiophene (v(HDS)) or cyclohexene (v(HYD) converted per second and per unit surface area of the used catalysts, assuming, in a first approximation, that the reactions are first order. The selectivity will also be reported (as v(HYD)/v(HDS)).

RESULTS

Specific Surface Area

The specific surface areas of the fresh and used catalysts are presented in Table 2. The specific surface area of the FeMoS-0.3-*T* sulfides decreases as the sulfiding temperature increases from 673 to 1073 K. For all sulfides, the specific surface area diminishes after catalytic work, especially for the MoS_2 and FeMoS-r-673 sulfides.

TABLE 2

Specific Surface Areas of the **Fresh** (S_0) and **Used** (S_1) Catalysts

Catalyst	S_0(m^2 g^{-1})	S_1(m^2 g^{-1})
FeMoS-0.15-673	50.0	31.0
FeMoS-0.30-673	68.6	33.0
FeMoS-0.30-773	34.0	23.0
FeMoS-0.30-873	25.1	16.0
FeMoS-0.30-1073	18.1	14.0
$Fe_{1-x}S$	7.8	3.2
MoS_2	51.8	29.0

X-ray Diffraction (XRD)

The XRD spectra of the fresh $Fe_{1-x}S$ and MoS_2 sulfides are shown in Fig. 1. The diffractogram of iron sulfide shows an XRD pattern (Fig. 1a) corresponding to the hexagonal pyrrhotite structure ($Fe_{1-x}S$). The XRD pattern of MoS_2 (Fig. 1b) is characteristic of a poorly crystallized MoS_2 exhibiting strong and broad (002) and (008) reflections as well as a broad envelope formed by the (100), (101), (102), (103), (006), and (105) reflections.

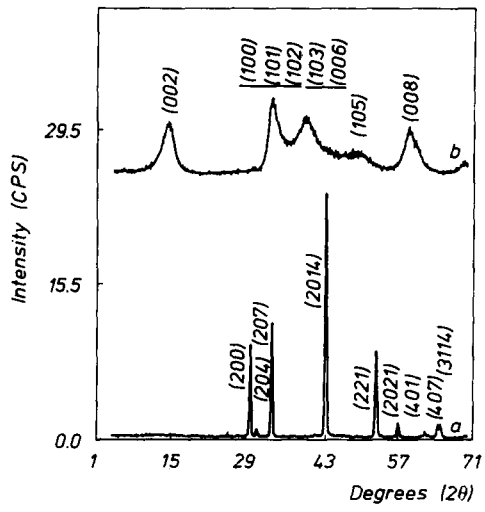

FIG. 1. XRD patterns of (a) $Fe_{1-x}S$ and (b) MoS_2.

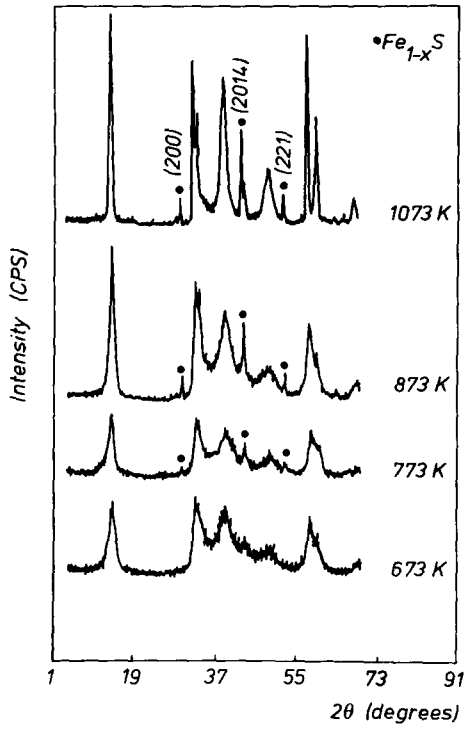

FIG. 2. XRD patterns of fresh FeMoS-0.30-*T* sulfides.

The XRD spectra of the **fresh** FeMoS-0.30-T sulfides are presented in Fig. 2. The XRD pattern of FeMoS-0.30-673 is characteristic of a poorly crystalized MoS_2-like phase. As the sulfidation temperature increases to 1073 K, the peaks due to the MoS_2 reflections become sharper and more intense, indicating an increasing crystallization of the MoS_2-like phase, and the peaks corresponding to the characteristic reflections of hexagonal pyrrhotite (ideal stoichiometry Fe_7S_8, actually $Fe_{1-x}S$) sulfide appear progressively.

The XRD pattern of the **used** FeMoS-0.30-*T* samples (T = 673, 873, and 1073 K) is shown in Fig. 3. In addition to the presence of molybdenum, always detected as an MoS_2-type phase, iron sulfide FeS (troilite) was detected in used catalysts (ASTM: 24-220A). Pyrrhotite ($Fe_{1-x}S$) is converted to FeS during reaction.

As the sulfidation temperature increases from 673 to 873 K, the thickness of the MoS_2 particles or slabs increases from 36.6 to 216 Å (Fig. 4). At 1073 K, (a), the particle size is about 5.9 times larger than that measured in FeMoS-873. The same trend is observed for the used FeMoS sulfides (b). Their particle size values are somewhat higher than those of the fresh samples.

Mössbauer Absorption Spectroscopy (MAS)

The MAS spectra of the **fresh** sulfides of the FeMoS-0.30-T series are presented in Fig. 5. The corresponding parameters, together with those of the FeMoS-0.15-673 sample, are reported in Table 3. The identification of the various iron sulfides, as indicated in Table 3, is explained in the discussion (Section 2.2). It suffices to mention here the presence of a central doublet Q1 (FeMoS), and a component in the form of a

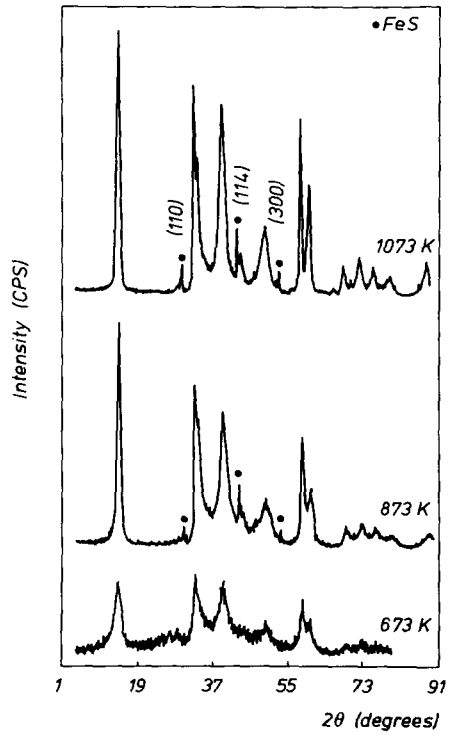

FIG. 3. XRD patterns of the used FeMoS-0.30-*T* sulfides.

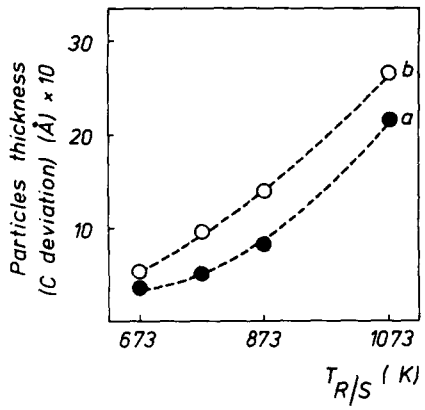

FIG. 4. Variation of the particle thickness (along the c-axis) of the MoS_2-type phase vs sulfidation temperatures: (a) fresh sulfides and (b) used sulfides.

six-line pattern (sextet H1, H2, H3) (hexagonal pyrrhotite). The Mössbauer spectra and parameters of the same samples, when **used**, are shown in Fig. 6 and Table 4, respectively. Note the presence of Q1 (FeMoS, which disappears above 673 K), of another doublet Q4 (pyrite, FeS_2), and a sextet Hb (troilite FeS). FeS_2 diminishes in favor of FeS when the sulfidation temperature increases.

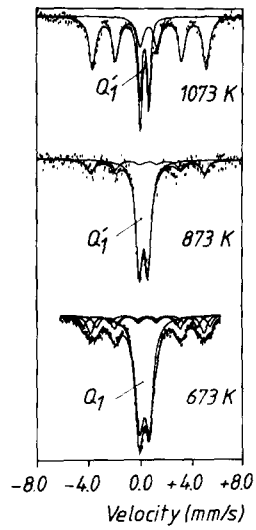

FIG. 5. MAS spectra of the fresh FeMoS-0.30-T sulfides.

Electrophoresis Measurements

The electrophoretic migration velocity of MoS_2, $Fe_{1-x}S$, and the FeMoS-0.30 sulfides are presented in Fig. 7. The isoelectric point (IEP) values of the MoS_2 and $Fe_{1-x}S$ were found to be 3.0 and 3.8, respectively. In the case of the FeMoS sulfide, only one kind of particle was observed, characterized by an IEP equal to 1.6. This value below the IEP of pure MoS_2 and $Fe_{1-x}S$.

DTA (TPDec Followed by TPO), TPS (Followed by TPO), TPR

Figure 8 shows the DTA curves of the thermal decomposition under argon (a,b) and the subsequent temperature oxidation (c,d) of the precursor of MoS_2 (a,c) and FeMoS (b,d) sulfides. Figure 9 reports the DTA curves of the temperature-programmed sulfidation-reduction (a,b) and the subsequent temperature-programmed oxidation (c,d,a) of the precursor of MoS_2 (a,c), $Fe_{(1-x)}S$ (d), and FeMoS (b,c) sulfides.

The temperature programmed reduction of the MoS_2 (a), $Fe_{(1-x)}S$ (b), FeMoS prepared at 673 (c), 873 (d), and 1073 K (e) are reported in Fig. 10.

X-ray photoelectron spectroscopy (XPS)

For the pure iron sulfide, the S $2p_{3/2}$ and Fe $2p_{3/2}$ measured BE were, respectively, 161 ± 0.2 and 710.3 ± 0.2 eV. The Fe/S intensity ratio is equal to 0.64. The Mo $3d_{5/2}$ and S 2 $p_{3/2}$ BE of MoS_2 are equal to 229.1 ± 0.2 and 161.9 ± 0.2 eV, respectively. The Mo/S XPS ratio, 0.48, is close to the bulk composition (0.5). The Mo $3d_{5/2}$ and S $2p_{3/2}$ BE of the FeMoS-0.30-T sulfides are independent of the sulfiding temperature (229.1 ± 0.2 and 162.1 ± 0.2 eV, respectively). The full width at half maximum (FWHM) of the Mo $3d_{5/2}$ and S $2p_{3/2}$ are also constant and both equal to 1.0 ± 0.2 eV.

The Fe $2p_{3/2}$ photoelectron lines for FeMoS-0.30-T are shown in Fig. 11. An increase of the sulfidation temperature from 673 to 1073 K brings about the disappearance of the peak at 708.9–709.0 eV and the progressive appearance of a peak character-

TABLE 3

Mössbauer Parameters of the **Fresh** FeMoS-*r*-*T*, at 298 K

Sulfidation (K) temp.	r	CS	QS (mm/s)	IS(Fe) (mm/s)	*r* (mm/s)	H_i (kOe)	ϕ	*I*%
	0.15	Q1	0.79	0.30	0.68	—	FeMoS	74.4
673	0.15	Q'Ha	0.53	0.32	0.24	—	"$Fe_{1-x}S$"	25.6
	0.30	Q1	0.74	0.33	0.77	—	FeMoS	59.1
	0.30	H1	0.00	0.59	0.60	303.5		10.8
	0.30	H2	0.00	0.61	0.60	255.4	Fe_7S_8	17.9
	0.30	H3	0.00	0.60	0.60	241.0		12.2
873	0.30	Q'1	0.67	0.31	0.59	—	$FeMoS/FeS_2$	75.8
	0.30	Ha	0.09	0.67	0.72	272.0	FeS	24.2
1073	0.30	Q'1	0.68	0.34	0.33	—	$FeMoS/FeS_2$	27.6
	0.30	Ha	0.09	0.70	0.59	272.3	FeS	72.4

Note. QS = quadrupole splitting, IS = isomer shift, H_i = internal magnetic field, *%I* = percentage of presumed phase *r* = full width at half maximum, CS is the characteristic signal, and ϕ is the corresponding phase.

ized by an Fe $2p_{3/2}$ BE equal to 710.1–710.3 eV.

The variation of the Fe/(Fe + Mo) XPS surface ratio with the sulfidation temperature for the series of the FeMoS-0.30-*T* is plotted in Fig. 12. At the lower sulfidation temperatures, the Fe/(Fe + Mo) ratio remains lower than the value corresponding to bulk composition (0.30); it decreases continuously.

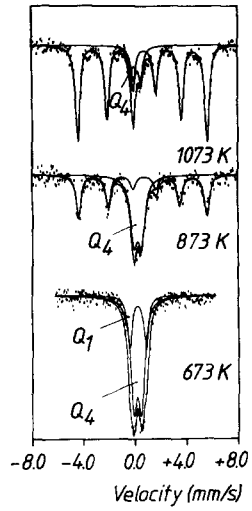

FIG. 6. MAS spectra of the used FeMoS-0.30-T sulfides.

Catalytic Activity

Figure 13 shows that the HDS and HYD activities become stable after 4 h. Intrinsic activities of the catalysts are shown in Table 5. FeMoS-0.15 and FeMoS-0.30 are slightly more active than unpromoted MoS_2 sulfide. Pure iron sulfide ($Fe_{1-x}S$) deactivated quickly and became almost completely inactive after 4 h operation. No significant difference was observed for the selectivity (vHYD/vHDS ratio) of the MoS_2 and FeMoS sulfides.

DISCUSSION

The discussion is in four sections. We first examine the arguments which prove that our samples, as a whole, are representative (and especially, that the FeMoS fresh series prepared at low temperature contains the "FeMoS phase"). This discussion is necessary if we wish to prove that our results give pertinent insight into the behaviour of the "FeMoS phase" as a function of the temperature of preparation and after catalytic reaction. The two following sections will then be devoted to the physico-chemical properties

TABLE 4

Mössbauer Parameters of the **Used** FeMoS-*r*-*T*, at 298 K

Sulfidation (K) temp.	r	CS	QS (mm/s)	IS(Fe) (mm/s)	*r* (mm/s)	H_i (kOe)	ϕ	*I*%
	0.15	Q1	1.03	0.32	0.52	—	FeMoS	53.3
673	0.15	Q3	0.46	0.33	0.54	—	"FeSx"	46.7
	0.30	Q1	1.27	0.32	0.43	—	FeMoS	27.4
	0.30	Q4	0.60	0.28	0.60	—	FeS_2	72.6
873	0.30	Q4	0.58	0.30	0.65	—	FeS_2	49.3
	0.30	Hb	0.16	0.68	0.47	309	FeS	50.7
1073	0.30	Q4	0.56	0.27	0.47	—	FeS_2	14.2
	0.30	Hb	0.16	0.74	0.41	311	FeS	85.7

Note. Symbols as in Table 3.

of fresh "FeMoS" samples obtained after different sulfiding temperatures and those of used catalysts. Then in the fourth section we will correlate catalytic activity with the results of the physico-chemical characterization, especially with the FeS_2 content, trying to explain the discrepancies observed in the literature.

1. Presence of "FeMoS"

This first section discusses the evidence showing that fresh catalysts prepared at 673 K exhibit the signals attributed to the so-called FeMoS phase, and that this FeMoS is distinct from known sulfides of iron or molybdenum.

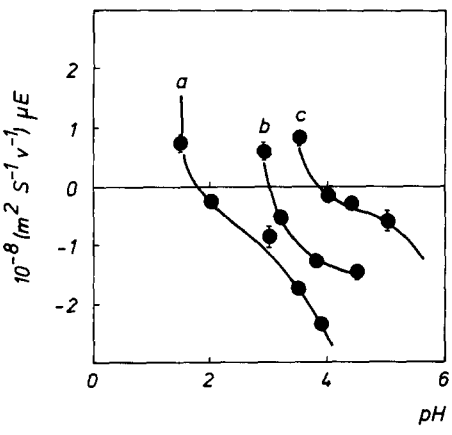

FIG. 7. Electrophoretic migration velocity vs pH curves: (a) FeMoS-0.30-673, (b) MoS_2, and (c) $Fe_{1-x}S$ sulfides.

The pure iron sulfide corresponds to hexagonal pyrrhotite as indicated by XRD and confirmed by the values of the isoelectric point (*30*) and XPS data (*38–40*). However, this pyrrhotite possibly departs from the ideal stoichiometry Fe_7S_8. The Fe/S ratio given by XPS, namely that corresponding to surface composition (Fe/S = 0.64), corresponds to an enrichment in sulfur compared to the bulk.

The characteristics of the precursor of MoS_2 (namely, a mixture of thio- and oxothiomolybdates), as determined by XRD, electrophoresis, and the thermoprogrammed experiments, correspond to the data in the literature (*31, 32, 41, 42*). The MoS_2 samples also exhibit characteristics corresponding to those in the literature (*30, 43–48*).

The characteristics of the FeMoS phase deserve careful discussion because the significance of our results depends on their identity with those attributed in the literature to this FeMoS species.

The main agruments come from MAS. The **fresh** FeMoS-0.15 and FeMoS-0.30 catalysts sulfided at 673 K give MAS spectra which can be deconvoluted into a central doublet (Q1) and a magnetic sextet (H1, H2, and H3). The Mössbauer parameters of the Q1 doublet are QS = 0.79 mm/s and IS = 0.33 mm/s. These values are close to those

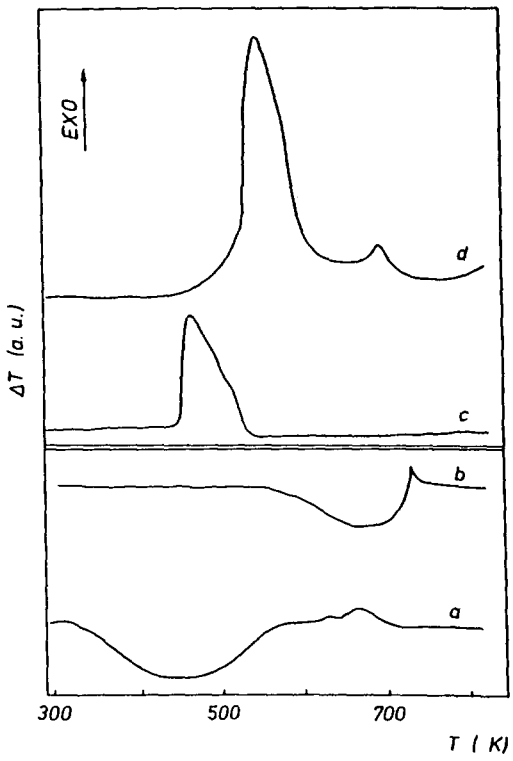

FIG. 8. DTA curves of the thermal decomposition under argon (a,b) and the subsequent temperature oxidation (c,d) of the precursor of the MoS_2 (a,c) and FeMoS (b,d) sulfides.

reported by Candia *et al.* (*15*) (QS = 0.83 mm/s, IS = 0.30 mm/s) and Qi *et al.* (*17*) (QS = 0.78 mm/s, IS = 0.35 mm/s). It is this doublet that the above authors attributed to iron in a special environment, which characterizes what is conventionally referred to as the "FeMoS phase." In a similar MAS study of the unsupported FeMo sulfide prepared by simple coprecipitation (CP), Ladrière *et al.* (*19*) reported (for the "FeMoS structure") the following values: QS = 0.99 – 1.22 mm/s and IS = 0.30 – 0.35 mm/s. The QS value was higher than the one cited above. This may be due to the use of a different preparation method. MAS allows a determination of the relative amount of "FeMoS phase" in the catalysts. It is found to be about 74.4 and 60% for our FeMoS-0.15 and 0.30, respectively.

The XRD spectrum of FeMoS-673 is found to be similar to that of amorphous MoS_2. A similar XRD spectrum has been obtained with CoMoS and NiMoS (*24, 25, 29*).

The TPDec of the FeMoS precursor did not show any exothermic effect at 450 K, as observed in the case of CoMoS (*24*) and NiMoS (*25*). This is due to the absence of NH_4NO_3 (which decomposes at about 450 K (*49*)), as shown by XRD. The broad weak endothermic peak, between 540 and 710 K, has been mentioned in the literature (*32*), but its origin was not explained. The important fact is that the TPDec peaks of the MoS_2 precursor are different from those

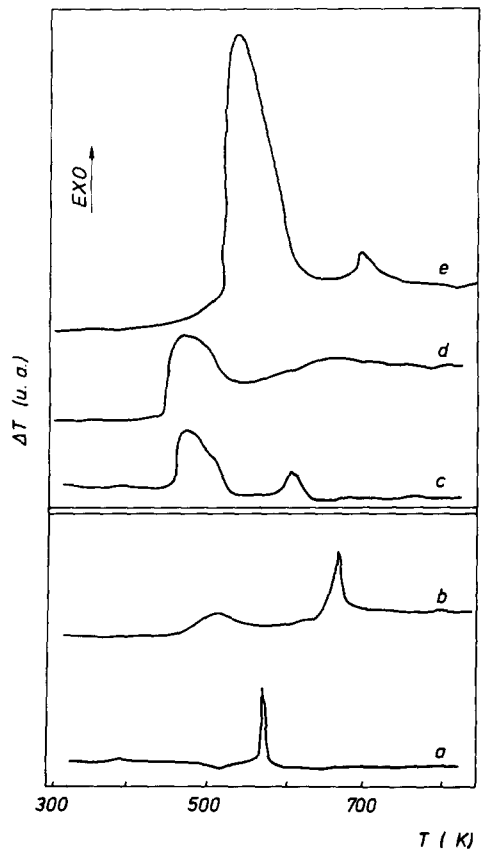

FIG. 9. DTA curves of the temperature-programmed sulfidation reduction (a,b) and the subsequent temperature-programmed oxidation (c,d,e) of the precursor of the MoS_2 (a,c) $Fe_{1-x}S$ (d), and FeMoS (b,e) sulfides.

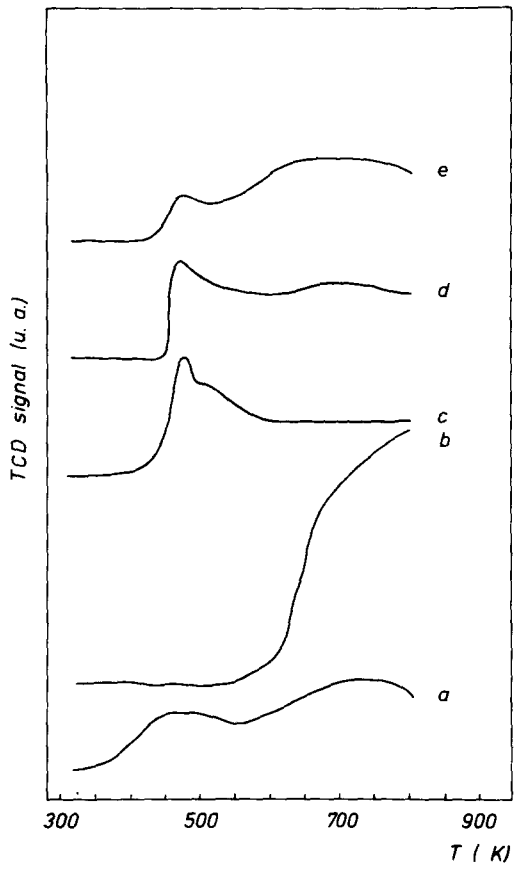

FIG. 10. TPR diagrams of (a) MoS_2, (b) $Fe_{1-x}S$, (c) FeMoS-0.30-673, (d) FeMoS-0.30-873, and (e) FeMoS-0.30-1073 sulfides.

of the FeMoS precursor (Fig. 8). According to Wu *et al.* (*32*), the broadening of the TPDec exothermic peak of the FeMoS precursor appearing at 710-730 K could be assigned to some interactions between Mo, Fe, and S. The most important DTA appears in TPO. For the two pure sulfides (MoS_2 and $Fe_{1-x}S$), the observed peaks could be attributed to the oxidation of sulfur into SO_2 and probably to the beginning of the oxidation of Mo and Fe to their highest oxidation state. The main TPO peak of FeMoS appears about 60 K higher than in the case of MoS_2 and $Fe_{1-x}S$ and is more intense. In addition, the TPO of FeMoS is completely different from the sum of the TPO contributions of MoS_2 and $Fe_{1-x}S$. This shows that Fe is associated with Mo and S in a different way compared to a simple mixture of MoS_2 and $Fe_{1-x}S$.

The TPS of the precursor of FeMoS (Fig. 9) shows that the sulfidation reaction takes place at a higher temperature (657 K) than that (576 K) corresponding to the sulfidation of MoS_2. This result indicates that, in the presence of iron, the sulfidation of the Mo-containing species is not easier, contrary to what is observed when the Mo was combined with Co or Ni (*24, 25, 31, 32*).

The TPR behaviour of the FeMoS-673 (Fig. 10) is different from that of the MoS_2. In particular, its TPR peak at 420–580 K is more intense and situated 40–60 K higher than the first exothermic peak of MoS_2 (but lower than the second exothermic peak). This can be explained by the fact that sulfur exposed on the MoS_2 edges is more weakly bound in the FeMoS structure than in the MoS_2, as reported by Göbölös *et al.* (*18*)

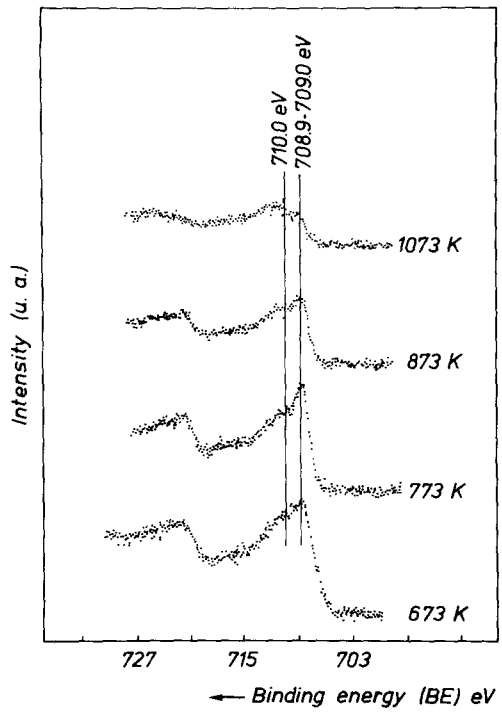

FIG. 11. XPS spectra of Fe $2p_{3/2}$ photoelectron lines of the fresh FeMoS-0.30-*T* sulfides.

TABLE 5

HDS and HYD Intrinsic Activity of the MoS_2, $Fe_{1-x}S$, FeMoS-0.15, and FeMoS-0.30 Sulfides Measured at $T = 573$ K

Catalyst	%Conv HYD	%Conv HDS	v(HYD) × 10^6 (mol s^{-1} m^{-2})	v(HDS) × 10^8 (mol s^{-1} m^{-2})	vHYD/vHDS
MoS_2	38.3	68.0	0.31	0.88	35
$Fe_{1-x}S$[a]	03.0	07.0	0.17	0.72	23
FeMoS-0.15	41.0	71.0	0.31	0.92	33
FeMoS-0.30-673	46.5	79.0	0.35	0.97	36
FeMoS-0.30-773	29.0	60.0	0.32	1.02	31
FeMoS-0.30-873	16.5	35	0.24	0.85	28
FeMoS-0.30-1073	6.5	14	0.12	0.44	27

[a] After 4 h on stream.

and Ladrière *et al.* (*19*). In addition also the TPR curve of FeMoS-673 did not correspond to the addition of the MoS_2 and $Fe_{1-x}S$ TPR patterns.

The presence of a large proportion of a special association, different from either MoS_2 or iron sulfides, in the samples obtained by the HSP method was also confirmed by the electrophoretic measurements. The fact that only one family of particles was observed indicates a very close association. The isoelectric point (IEP) value of the FeMo sulfide was found to be different from that of the MoS_2 and $Fe_{1-x}S$ and equal to 1.6. This IEP value (almost identical to those observed for CoMoS and NiMoS, namely, 1.5) is in good agreement with that reported by Göbölös *et al.* (*30*) for the "FeMoS phase."

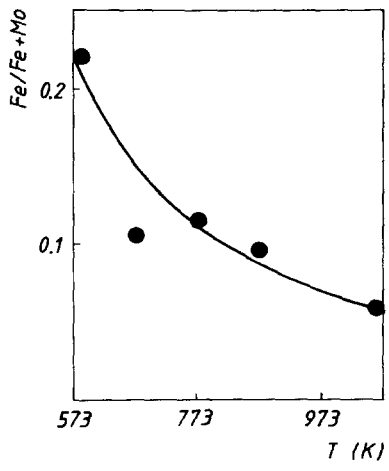

FIG. 12. Fe/(Fe + Mo) surface atomic ratio by XPS vs sulfidation temperatures.

In conclusion, our "FeMoS" samples sulfided in standard conditions, namely, at 400°C under H_2/H_2S (15% H_2S), show comparable behaviour to those reported by other authors. The data obtained with them (in particular stability and catalyst activity) can thus be taken as representative of the behaviour of the "FeMoS" species.

2. *Characterization of the* ***Fresh*** *FeMoS-0.30-T Series Sulfided at Different Temperatures*

The FeMoS-0.30-T catalysts suffer increasing losses of surface area when the sulfidation temperature is raised from 673 to 1073 K (see Table 2). Figure 4 suggests that the increase of the size of the MoS_2-like phase crystallites is the main reason for this.

Although the content of FeMo-0.15-673 in FeMoS is 75%, FeMo-0.30-673 contains only about 60% of it. In addition to it, another iron sulfide species is detected. It is characterized by magnetic sextets (H1, H2, H3). Their hyperfield (Hi1, Hi2, Hi3) and the corresponding IS values are in good agreement with those reported in Refs. (*19*) and (*50*) for monoclinic pyrrhotite (ideal formula: Fe_7S_8), although XRD indicates that

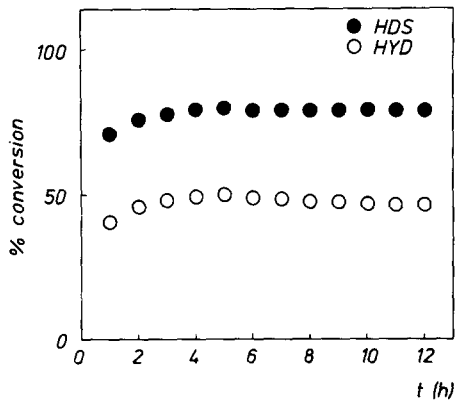

FIG. 13. Variation of the catalytic activities of FeMoS-0.30-673 with the time of reaction.

it is actually amorphous and probably nonstoichiometric in our catalyst ($Fe_{1-x}S$). In the case of FeMoS-0.15, the doublet Q'Ha, because of its high IS value, may be attributed to iron sulfide with a high ionic character. We speculatively propose that this iron sulfide could be superparamagnetic pyrrhotite.

For both FeMoS-0.30-873 and FeMoS-0.30-1073, the IS value was found to be similar to that in FeMoS-0.30-673. However, the QS value undergoes a slight decrease with the sulfidation temperature (see Table 3). According to Qi *et al.* (*17*), the doublet Q'1 could correspond to iron in "FeMoS phase". However, some studies (*11, 51*) reported a QS value of 0.614 mm/s and IS = 0.314 mm/s for pure pyrite FeS_2. In spite of this discrepancy in the literature, the doublet Q'1 can probably be attributed mainly to FeS_2, though "FeMoS structure" may also be present. An agrument in favor of the first interpretation is that FeS_2 was detected in the sample named $Fe_{1-x}S$ by XRD (*52*). Presumably because it is in small amounts, FeS_2 could not be detected by XRD in our FeMo sulfides. The MAS parameters of the six-line pattern (Ha) (see Table 2) were in perfect accordance with those cited in the references (*4, 53*) for the hexagonal pyrrhotite ($Fe_{1-x}S$) over a wide range of nonstoichiometry (Fe_7S_8 to $Fe_7S_{8.75}$). Well-crystallised $Fe_{1-x}S$ was detected by XRD in these sulfides. The presence of hexagonal pyrrhotite confirms the findings of several groups (*4, 17, 20*). The explanation would be that MoS_2 can stabilise pyrite in conditions where $Fe_{1-x}S$ phase is theoretically the only thermodynamically stable phase.

The relative intensity of Ha increases at the expense of Q'1, when the sulfidation temperature increases from 873 to 1073 K, indicating the partial transformation of (FeS_2 + "FeMoS phase") into $Fe_{1-x}S$. The amount of (FeS_2 + "FeMoS") decreases from 75.8% at 873 K to 27.6% at 1073 K, whereas that of $Fe_{1-x}S$ increases from 24.2% at 873 K up to 72.4% at 1073 K. The TPR and XRD results agree with these data, especially the increase of pyrrhotite when the sulfiding temperature increases. In the TPR analysis of FeMoS-0.30-*T*, the intensive broad band, characteristic of the removal of sulfur, probably comes from iron sulfide rather than from molybdenum sulfide (compare Figs. 10a and 10b with 10c–10e). It increases with the sulfidation temperature. The partial segregation of iron from the "FeMoS phase" (iron dispersed on the edges of MoS_2) as $Fe_{1-x}S$ goes along with the increase of crystallinity of the MoS_2-like phase induced by higher sulfidation temperature. Indeed, according to Topsøe *et al.* (*14*), a high sulfidation temperature provokes a lowering of the MoS_2 edge area, and, as Fe can no longer be accommodated on the edges, it segregates from the "FeMoS phase."

XPS shows that at least two iron-containing species are present in the FeMoS sulfides (see Fig. 11). One of these is characterized by an Fe $2p_{3/2}$ BE value equal to 708.9–709.1 eV. This BE is higher than those (706.6 and 706.4 eV) of the FeS_2 sulfides (pyrite and marcasite, respectively) and lower than 711.2 eV, characteristic of FeS (troilite) (*54*). There is little information in the literature about the nature of this species. Based on the MAS and XRD results, we propose that this Fe species might be attributed to sulfided iron associated with MoS_2 in the FeMoS catalyst. The intensity

of the corresponding XPS peak diminishes as the sulfidation temperature increases. The other species was characterized by an Fe $2p_{3/2}$ BE equal to 7.10 ± 0.2 eV.This corresponds perfectly to pyrrhotite $Fe_{1-x}S$. In agreement with the MAS and XRD results, the intensity of this peak increases with the sulfidation temperature.

The Fe/(Fe + Mo) XPS ratio (0.20) is lower than the bulk composition (0.30). This could be due to a coverage of the iron sulfides by MoS_2 as reported by Groot (*55*). Adopting this interpretation would imply that the location of Fe in FeMoS is not restricted to the edges and corners of the MoS_2 slabs, but corresponds also to the interior of MoS_2. However, a much simpler explanation is that some segregation of FeS_x from FeMoS has already taken place, and that this FeS_x is poorly dispersed and hence emits proportionally fewer photoelectrons. The Fe/(Fe + Mo) ratio decreases continuously. The interpretation is almost certainly that the amount of iron coming from "FeMoS phase" to form pure iron sulfide increases, and that the corresponding crystallites expose a smaller area for the escape of Fe $2p_{3/2}$ electrons than Fe in FeMoS.

3. *Stability of the "FeMoS Phase" during the Catalytic Reactions*

The catalysts lose surface area during activity tests (Table 2). This loss is substantial for FeMoS-0.30-673, namely, more than 50%. This may be due, in part, to some coke deposition (*56*), but crystal growth certainly plays an important role: this is shown by XRD (see Fig. 4). This corresponds to other observations in the literature (*57*).

The amounts of "FeMoS phase" and pure iron sulfide in the fresh and used FeMoS-0.30 or FeMoS-0.15-673 catalysts, taken from the results presented, are shown, respectively, in Figs. 14 and 15. The amount of "FeMoS phase" in FeMoS catalysts decreases after catalytic work, and, correlatively, the amount of pure iron sulfide increases. These results confirm that iron segregates from the "FeMoS phase" at medium-high H_2 pressure, to form pure iron sulfide. This phenomenon is similar to that observed by Breysse *et al.* (*23*), who proved that Co in the similar "CoMoS phase" structure is highly sensitive to H_2 and that the Co MES signal progressively becomes very close to that corresponding to Co_9S_8. Segregation phenomena in "CoMoS" at a high hydrogen pressure have also been reported by Candia *et al.* (*22*). Taking into account the same location of Fe on MoS_2 edges as compared with that of Co in "CoMoS" phase (*58*), one may expect comparable behavior of both sulfided systems even though their electronic properties are different (*8, 9*) leading to different strength of the metal-sulfur bond.

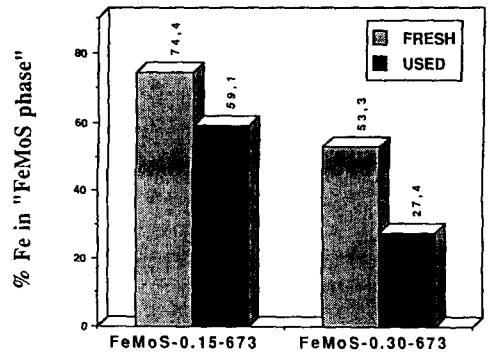

FIG. 14. Percentage of Fe in "FeMoS phase" in the **fresh** and **used** FeMoS sulfide.

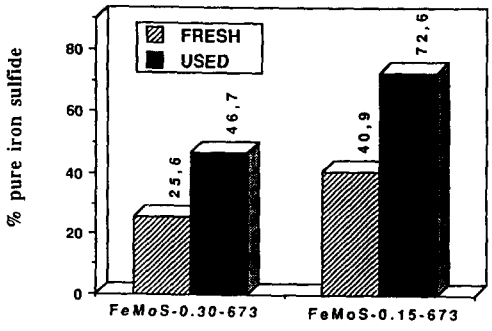

FIG. 15. Percentage of Fe in pure iron sulfide in the **fresh** and **used** FeMoS sulfide.

Mössbauer spectroscopy (Table 4) shows that FeMoS-0.30-673 undergoes a significant change during use. It should be remembered that two phases are present in the catalyst, namely "FeMoS" and $Fe_{1-x}S$ (Table 4). However, the QS value (1.27 mm/s) of the Q1 signal is higher than that (0.79 mm/s) of the fresh FeMo catalyst. The "FeMoS phase" of the used catalysts has the same MAS parameters as those reported by Ladrière *et al.* (*19*) in their study of a series of catalysts. These authors attributed this doublet to the so-called "FeMoS phase." This change of the QS parameters may be due to a change in the crystallinity of the catalysts: the explanation would be consistent with results of Ladrière *et al.* (*19*). The doublet Q4 was attributed to FeS_2 in accordance with the literature (*59–61*). The monoclinic pyrrhotite present in fresh FeMoS-673 became transformed, during catalytic test, into FeS_2 (*11, 52*). FeS_2 ($\cong$73%) is formed, for one part, from Fe_7S_8 (40%), and the FeMoS phase for the difference ($\cong$33%).

In the case of the FeMoS-0.30-873 and FeMoS-0.30-1073, the best fitting of the MAS spectra shows the presence of two compounds which are characterized by the doublet Q4 and a magnetic sextet (Hb). The Mössbauer parameters of the Hb sextet are those of troilite (FeS) (*53, 62*), and correspond to near stoichiometric compounds (*51, 63, 64*). Troilite FeS was the only pure iron sulfide which could be detected by XRD. Increasing the sulfidation temperature caused a considerable decrease of the concentration of the FeS_2 (from 72.6% at 673 K to 14.2% at 1073 K) whereas that of FeS increased (from 50.7% at 873 K to 85.7% at 1073 K). Troilite is the thermodynamically stable iron sulfide under our experimental conditions (*65*). This is in good agreement with the work of Smith *et al.* (*66*), who showed that in HDS of thiophene with H_2, both pyrite (FeS_2) and pyrrhotite ($Fe_{1-x}S$) were converted into troilite (FeS). In their case also, part of the FeS_2 remained untransformed.

The FeMoS species becomes completely transformed into pure iron sulfides. This situation is similar to that of the "CoMoS or NiMoS" phases which are poorly stable under the medium-high pressure conditions in the reactor and decompose into pure sulfides (*11, 22, 24, 25, 29*). It has been shown that the mixed "CoMoS" or "NiMoS" phases act as a precursor, and, either on high-temperature activation or during high-pressure catalytic activity run, segregate, leading to biphasic catalysts in which Co_9S_8 or Ni_2S_3 are formed at the expense of the mixed phase.

The diminution of the number of Fe atoms associated with "FeMoS" after catalytic work does not seem to have the same origin as the phenomenon observed when high sulfidation temperatures are used. In the above discussion of this latter effect, we attributed the segregation phenomenon of pure iron sulfides mainly to the diminution of the edge surface area of MoS_2 (namely, a diminution of the number of the sites available for "decoration"). During catalytic use, the thickness of the MoS_2 crystallites along the *c*-axis changes much less (from approximately 36 to 53 Å) than when the sulfiding temperature varies from 673 to 1073 K (from about 36 to more than 215 Å). Another origin for the segregation must exist. The tendency of the iron atoms associated with Mo in the "FeMoS phase" to segregate is probably linked fundamentally to the fragility of the attachment of Fe to the MoS_2 structure. One possible explanation would come from the proposal of Groot (*55*), who, on the basis of XPS measurements, supposes that Fe, Mo, and S are present as an MoS_2–FeS mosaic, where a part of FeS is covered by MoS_2. If we accept this proposed structure, the conclusion would be that, under hydrogen pressure, this structure decomposes into molybdenum and iron sulfides. However, one could also simply conclude that the reducing conditions prevailing during catalytic work bring about the breaking of the bonds attaching Fe to the MoS_2 structure.

4. Catalytic Activity

There are conflicting views in the literature with respect to the HDS activity of pure iron sulfides. Pecoraro and Chianelli (*8*) have reported that dibenzothiophene HDS activity of pure iron sulfide (designated as FeS_x), measured at 673 K and under a pressure of 3.1 MPa, is much lower than that of MoS_2. Ramselaar *et al.* (*12*) have studied the thiophene HDS activity of Fe/C, measured after 2 h on stream under atmospheric pressure. They found that the HDS activity decreased markedly when the iron content increased. In the work of Groot *et al.* (*38*), iron supported on carbon was found to have a higher thiophene HDS activity and a lower butene HYD activity than MoS_2. In the present work the initial HDS and HYD activity were found to be equal to 5.8×10^{-8} and 1.39×10^{-6} mol s^{-1} m^{-2}, respectively. In spite of the low surface area of $Fe_{1-x}S$ (Table 2), activities are higher than those of the FeMo sulfide. However, we also found that $Fe_{1-x}S$ sulfide deactivated very rapidly and its activity became negligible after 4 h on stream. The loss of activity must be explained by phase transition of the $Fe_{1-x}S$ into FeS during reaction, and, possibly, coke deposition. Our results explain the discrepancies found in the literature. The activity of $Fe_{1-x}S$ is only significant with the starting material, but becomes negligible after some time under the reaction conditions.

Visser *et al.* (*39*) attributed the weak iron promoting effect to the presence of a "FeMoS phase." They detected this species, together with $Fe_{1-x}S$ and FeS_2, by Mössbauer spectroscopy in the fresh catalyst, but did not mention any involvement of the pure iron sulfides in the promoting effect. The presence of FeS_2 in used unsupported FeMo catalyst has been reported in other publications (*12, 19*). This sulfide was found to be capable of bringing about hydrogenolysis (*20*). In the work of Göbölös *et al.* (*18*), the HDS activity of the unsupported FeMo catalyst was found to decrease as the amount of FeS_2 in the used catalyst decreased. In our case, both used FeMoS-0.15 and 0.30, sulfided at 673 K, were composed of some remaining "FeMoS phase" and pure iron sulfide $Fe_{1-x}S$ (a total of about 15.3 and 25%, in the case of FeMoS-0.15 and FeMoS-0.30, respectively). The active phase seems to consist of a mixture of pure iron sulfide (FeS_2, FeS) and MoS_2-like phase (MoS_2 and "FeMoS"). In spite of the high amount of "FeMoS phase" in our FeMoS-0.15, its activity was found to be lower than that of FeMoS-0.30, which contains much lower amounts of the "FeMoS phase." This implies that the HDS activity is not proportional to the amount of the "FeMoS phase" in the catalyst and suggests that it may also be related to the presence of pure iron sulfide.

The HDS and HYD intrinsic activities are only moderately affected when the sulfidation temperature increases from 673 to 773 K (see Table 5), in spite of substantial changes in the texture of the catalysts (strong loss of surface area from 68.6 to 34.0 m^2 g^{-1} and increase of the thickness of the MoS_2 crystallites, as shown in Fig. 4). Above 773 K, the activities for both reactions diminish continuously. The FeMoS-0.30-T samples corresponding to $T = 873$ and 1073 K practically do not contain any "FeMoS phase." Nevertheless, they possess an appreciable intrinsic catalytic activity, especially FeMoS-873. This implies that the mixture of MoS_2, FeS, and FeS_2, without the "FeMoS phase", is active. The continuous decrease of the intrinsic activity may be due principally to the progressive crystallisation of the catalyst during reaction, corresponding to a diminution of the edge area of MoS_2 and accordingly of the number of Mo active sites. The decrease of the amount of FeS_2 varies practically in the same manner as the decrease of activity.

In the literature, a positive correlation between the amount of the "FeMoS phase" in fresh catalysts and activity has been reported (*12, 17*).

Our results do not show this sort of correlation: no "FeMoS phase" was detected in

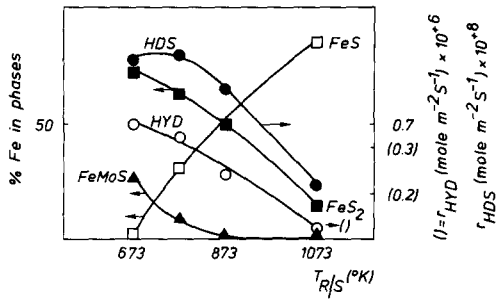

FIG. 16. Correlation between HDS and HYD activities of FeMoS-0.30-*T* and the amounts of the iron-containing species present in the **used** FeMoS catalysts.

used FeMo catalysts sulfided at 873 and 1073 K, in spite of the fact that they retain (especially FeMoS-0.30-873) about 80% of the intrinsic activity of FeMoS-0.30-673 (Fig. 13). Figure 16 suggests that FeS_2 plays some role: there is a parallelism between the variation of the HDS and HYD activities and the amount of FeS_2 present in the used catalysts.

CONCLUSIONS

1. Iron is a weak promoter for hydrodesulfurisation (HDS) in unsupported FeMo catalyst.

2. Two iron species exist in **fresh** FeMo sulfide prepared by the HSP method, namely, the "FeMoS phase" and pyrrhotite $Fe_{1-x}S$.

3. An increase of the sulfidation temperature induces considerable textural and structural modifications of the unsupported FeMo sulfide. In particular:

—an increase of the pyrrhotite content

—the FeS_2 and sulfided Fe in "FeMoS phase" are partially converted into FeS (troilite), which is the stable phase under reaction conditions

—in the same way as for the Co(Ni) MoS phase partial segregation leading to biphasic catalyst is obtained by sulfidation at high temperature

4. Three iron species could be detected in the **used** FeMo sulfide: these were the "FeMoS phase," FeS_2, and FeS. The concentration of troilite FeS increases, as for catalysts initially sulfided at increasing temperatures.

5. The "FeMoS phase" is unstable during the catalytic reaction at 3 MPa total pressure and 573 K. This unsupported catalyst presents the same behaviour as the "CoMoS" or "NiMoS" phase.

6. The catalytic activity does not correlate with the percentage of the "FeMoS phase" in the catalyst. The HDS activity decreases as the amount of FeS_2 decreases and an optimal concentration of the mixture ((FeS_2 or/ and FeS) + FeMoS phase) seems suitable to obtain high HDS activity.

ACKNOWLEDGMENTS

Financial support by the "Ministère de la Politique Scientifique" (Belgium) in the frame of the national "catalysis" program "Pole d'Attraction Interuniversitaire" is gratefully acknowledged, especially for a fellowship to H.M. One of us (M.K.) gratefully acknowledges financial support from the Faculty of Sciences, Mohamed 1st University, Oujda. We also thank Dr. J. Naud for XRD measurements and Professor G. Froment and Mr. M. Genet for useful discussions.

REFERENCES

1. Garg, D., and Givens, E. N., *Ind. Eng. Chem. Process Des. Dev.* **21,** 113 (1982).
2. Stohl, F. V. *Fuel* **62,** 122 (1983).
3. Yunes, S., Thakur, D. S., Grange, P., and Delmon, B., *in* "Catalysts in Petroleum Refining 1989" (D. L. Trimm *et al.*, Eds.), p. 317. Elsevier, Amsterdam.
4. Vaishnava, P. P., Montano, P. A., Tischer, R. E., and Pollack, S. S., *J. Catal.* **78,** 454 (1982).
5. Montano, P. A., and Granoff, B., *Fuel* **59,** 214 (1980).
6. Thakur, D. S., Grange, P., and Delmon, B., *J. Less-Common Met.* **64,** 201 (1979).
7. Göbölös, S. Wu, Q. André, O., Delannay, F., and Delmon, B., *J. Chem. Soc. Faraday Trans. 1,* **82,** 2423 (1986).
8. Pecoraro, T. A., and Chianelli, R. R., *J. Catal.* **67,** 430 (1981).
9. Harris, S., and Chianelli, R. R., *J. Catal.* **86,** 400 (1984).
10. Harris, S., and Chianelli, R. R., *J. Catal.* **98,** 17 (1986).
11. Ramselaar, W. L. T. M., Craje, M. W. H., Gerkema, E., De Beer, V. H. J., and van der Kraan, *Bull. Soc. Chim. Belg.* **96**(11–12), 931 (1987).
12. Ramselaar, W. L. T. M., Ph.D. thesis, Leiden, Germany, 1988.

13. Topsøe, H., Clausen, B. S., Candia, R., Wivel, C., and Mørup, S., *Bull. Soc. Chim. Belg.* **90,** 1189 (1981).
14. Topsøe, H., Candia, R., Topsøe, N.-Y., and Clausen, B. S., *Bull. Soc. Chim. Belg.* **93** (8–9), 783 (1984).
15. Candia, R., Clausen, B. S., and Topsøe, H., *J. Catal.* **77,** 564 (1982).
16. Clausen, B. S., Mørup, S., Topsøe, H., and Candia, R., *J. Phys. Colloq.* **C6-249,** 146 (1976).
17. Qi, H., Yang, X., Gu, Y., Zhu, C., Ren, J., and Zhou, N., *Guihua Xuebao* **5,** 146 (1984).
18. Göbölös, S., Wu, Q., Delannay, F., Grange, P., Delmon, B., and Ladrière, J., *Polyhedron* **5,** 219 (1986).
19. Ladrière, J., Göbölös, S., Thakur, D. S., Wu, Q., and Delmon, B., *Hyperfine Interact.* **28,** 907 (1986).
20. Thakur, D. S., *J. Catal.* **94,** 310 (1985).
21. Brooks, D. G., Guin, J. A., Custis, C. W., and Placek, T. D., *Ind. Eng. Chem. Process Des. Dev.* **22,** 343 (1983).
22. Candia, R., Topsøe H., and Clausen, B. S., *in* "9th Iberoamerican Symposium on Catalysis, July 16–21, 1984, Lisboa, Portugal," Vol. 1, p. 211.
23. Breysse, M., Frety, R., Benaichouba, B., and Bussière, P. *Radiochem. Radioanal. Lett.* **B59,** 265 (1983).
24. Karroua, M., Grange, P., and Delmon, B., *Appl. Catal.* **50**(3), L5 (1989).
25. Karroua, M., Ph.D. thesis, Louvain-la-Neuve, Belgium 1990.
26. Ledoux, M. J., Michaux, O., Agostini, G., and Panissod, P., *J. Catal.*, **102,** 275 (1986).
27. Ledoux, M. J., Michaux, O., Agostini, G., and Panissod, P., *J. Catal.*, **93,** 189 (1985).
28. Ledoux, M. J., Maire, G., Hantzer, S., and Michaux, O., *in* "Proceedings, 9th International Congress on Catalysis, Calgary, 1988" (M. J. Phillips and M. J. Ternan, Eds.), p. 74. Chemical Institute of Canada, Ottawa, 1988.
29. Candia, R., Clausen, B. S., and Topsøe, H., *Bull. Soc. Chim. Belg.* **90,** 1225 (1981).
30. Göbölös, S., Wu, Q., and Delmon, B., *Appl. Catal.* **13,** 89 (1984).
31. Wu, Q., Göbölös, S., Delannay, F., and Delmon, B., *in* "Reactivity of Solids" (P. Barret and L. C. Dufour, Eds.), p. 1067. Elsevier, Amsterdam, 1985.
32. Wu, Q., Göbölös, S., Grange, P., and Delannay, F., *Thermochim. Acta.* **81,** 219 (1984).
33. Klug, H. P., and Alexander, L. E., "X-Ray Diffraction Procedures," p. 419. Wiley, New York, 1954.
34. Parks, G. A., *Chem. Rev.* **65,** 177 (1965).
35. Wagner, D. S., Davis, L. E., Zeller, M. V., Taylor, J. A., Ruymond, R. H., and Cale, L. H. *Surf. Interface Anal.* **3,** 211 (1981).
36. Scofield, J. H., *J. Electron. Spectrosc. Relat. Phenom.* **8,** 129 (1976).
37. Delannay, F., Damon, J. P., Masson, J., and Delmon, B., *Appl. Catal.* **4,** 169 (1982).
38. Groot, C. K., van der Kraan, A. M., De Beer, V. H. J., Prins, R., *Bull. Soc. Chim. Belg.* **93**(8–9), 707 (1984).
39. Vissers, J. P. R., Groot, C. K., van Oers, E. M., De Beer, V. H. J., and Prins, R., *Bull. Soc. Chim. Belg.* **93**(8–9), 813 (1984).
40. Carver, J. C., and Schweidzer, G. K., *J. Chem. Phys.* **57,** 973 (1972).
41. Prasad, T. P., Diemann, E., and Müller, A., *J. Inorg. Nuc. Chem.* **35,** 1893 (1973).
42. Rode, E. Ya., and Lebedev, B. A., *Russ. J. Inorg. Chem.* **6,** 608 (1961).
43. Chianelli, R. R., Prestridge, E. B., Pecoraro, A. T., and de Neufville, J. P., *Science* **203,** 1107 (1979).
44. Breysse, M., Frety, R., Vrinat, M., Grange, P., and Genet, M., *Appl. Catal.* **12,** 165 (1984).
45. Nag, N. K., Frenkel, D., Moulijn, J. A., and Gates, B. C., *J. Catal.* **66,** 161 (1980).
46. Massoth, F. E., Chang, K. S., and Ramachandran, R. *Fuel Process. Technol.* **66,** 161 (1980).
47. Kazstelan, S., Jalowiecki, L., Wambeke, A., Grimblot, J., and Bonnelle, J. P., *Bull. Soc. Chim. Belg.* **96,** 1003 (1987).
48. Hoolds, R. C., Moyes, R. B., and Wells, P. B., *Bull. Soc. Chim. Belg.* **93,** 673 (1984).
49. Inoue, L., Kurusu, A., Wakamatsu, H., and Inui, T., *Appl. Catal.* **32,** 203 (1987).
50. Levinson, L. M., and Treves, D., *J. Phys. Solids* **29,** 2227 (1968).
51. Gosselin, J. R., Townsend, M.G., Tremblay, R. J., and Webster, A. H., *J. Solid State Chem.* **17,** 43 (1976).
52. Kouchonova, G. N., Ustanevich, M. Yu, Tomlov, S. B., and Cser, L., *Phys. Status Solidi* **31,** 141 (1970).
53. Ono, B. K., Ito, A., and Hirahara, E., *J. Phys. Soc. Jpn.* **17,** 1615 (1962).
54. Binder, H., Z. Naturforsch. **28b,** 255 (1973).
55. Groot, C. K., Ph.D. thesis, University of Eindhoven, 1984.
56. Zaidman, N. M., Osechkin, D. B., Gladovskaya, M. F., and Martynova, E. N., *Khim. Tekhnol. Topl. Masel* **6,** 25 (1961).
57. Furimsky, E., and Amberg, C. H., *Can. J. Chem.* **53,** 3567 (1975).
58. Mørup, S., Clausen, B. S., and Topsøe, H., *J. Phys. (Paris)* **40,** C2-88 (1979).
59. Morice, J. A., Rees, L. V. C., and Richard, D. T., *J. Inorg. Nucl. Chem.* **31,** 3797 (1969).
60. Sannuel, B., Fonkla, L., III, and Gathes, L. *Acta. Crystallogr.* **A32,** 529 (1976).
61. Knasy, J., Panek, T. J., and Szuszkiewicz, M., *J. Phys. Solid State* **17,** 1585 (1984).
62. Ioffe, P. A., Tsemekhan, L. S. H., and Vaisburd, S. E., *Dokl. Akad. Nauk. SSSR* **228,** 92, (1976).

63. Thiel, R. C., and van den Berg, C.B., *Phys. Status. Solidi,* **29,** 837 (1968).
64. Spender, M. R., Coey, J. M. D., and Morrish, A. H., *Can. J. Phys.* **50,** 2313 (1972).
65. Okutaui, T., Yokoyama, S., Maekawa, Y., Furuichi, R., and Ishii, T. *Ind. Eng. Chem. Process Des. Dev.* **22,** 306 (1983).
66. Smith, G. V., Hinkley, C. C. Zahra, O., Nishizawa, T., Saporoschenko, M., and Shiley, R. H., *J. Catal.* **78,** 262 (1982).